


# Accumulation of long-chain bases in yeast promotes their conversion to a long-chain base vinyl ether<sup>S</sup>

Fernando Martínez-Montañés,<sup>1,\*</sup> Museer A. Lone,<sup>2,\*</sup> Fong-Fu Hsu,<sup>†</sup> and Roger Schneider<sup>3,\*</sup>

Department of Biology,\* University of Fribourg, 1700 Fribourg, Switzerland; and Department of Internal Medicine,<sup>†</sup> Washington University School of Medicine, St. Louis, MO 63110

**Abstract** Long-chain bases (LCBs) are the precursors to ceramide and sphingolipids in eukaryotic cells. They are formed by the action of serine palmitoyl-CoA transferase (SPT), a complex of integral membrane proteins located in the endoplasmic reticulum. SPT activity is negatively regulated by Orm proteins to prevent the toxic overaccumulation of LCBs. Here we show that overaccumulation of LCBs in yeast results in their conversion to a hitherto undescribed LCB derivative, an LCB vinyl ether. The LCB vinyl ether is predominantly formed from phytosphingosine (PHS) as revealed by conversion of odd chain length tracers C17-dihydrosphingosine and C17-PHS into the corresponding LCB vinyl ether derivative. PHS vinyl ether formation depends on ongoing acetyl-CoA synthesis, and its levels are elevated when the LCB degradative pathway is blocked by deletion of the major LCB kinase, *LCB4*, or the LCB phosphate lyase, *DPL1*. PHS vinyl ether formation thus appears to constitute a shunt for the LCB phosphate- and lyase-dependent degradation of LCBs.  Consistent with a role of PHS vinyl ether formation in LCB detoxification, the lipid is efficiently exported from the cells.—Martínez-Montañés, F., M. A. Lone, F-F. Hsu, and R. Schneider. **Accumulation of long-chain bases in yeast promotes their conversion to a long-chain base vinyl ether.** *J. Lipid Res.* 2016. 57: 2040–2050.

**Supplementary key words** ceramide • sphingolipids • *Saccharomyces cerevisiae* • mass spectrometry

Sphingolipids are an essential class of lipids greatly enriched in the plasma membrane of eukaryotic cells. They have been implicated in the formation and maintenance of lateral membrane domains, important for protein sorting and signaling along the compartments of the secretory pathway. Apart from these structural roles, their biosynthetic precursor and intermediates, such as long-chain bases (LCBs) and ceramide, exert important signaling functions to coordinate complex processes, for example, cell cycle progression, apoptosis, and inflammation. Hence, the synthesis and turnover of these lipids must be precisely controlled (1–3).

This work was supported by the canton of Fribourg, the Novartis Foundation (14A35), and the Swiss National Science Foundation (31003A\_153416). The Washington University mass spectrometry facility is supported by U.S. Public Health Service Grants P41-GM103422, P60-DK-20579, and P30-DK56341.

Manuscript received 11 July 2016 and in revised form 9 August 2016.

Published, JLR Papers in Press, August 25, 2016  
DOI 10.1194/jlr.M070748

Sphingolipid synthesis starts in the endoplasmic reticulum (ER), where serine palmitoyl-CoA transferase (SPT) catalyzes the first step in formation of LCBs (4). Variations in chain length of the condensing acyl-CoA and the incorporation of alternative amino acids can result in the synthesis of a chemically heterogeneous set of sphingoid bases (5, 6). The activity of SPT, the rate-limiting enzyme of the pathway, is negatively regulated by Orm proteins, conserved integral ER membrane proteins whose phosphorylation relieves inhibition of SPT activity (7, 8). Kinases that phosphorylate Orm proteins thus integrate multiple signals to maintain sphingolipid homeostasis, including heat and ER stress, and availability of nutrients (9–13).

The major LCBs in yeast are dihydrosphingosine (DHS) and phytosphingosine (PHS), which upon ceramide formation condense with a CoA-activated C26 very long-chain fatty acid (14, 15). This reaction is catalyzed by the ER-localized ceramide synthase (CerS). Upon transport to the Golgi apparatus, ceramides are converted to a set of complex sphingolipids: inositol phosphorylceramide, mannosylinositol phosphorylceramide, and mannosyl-diinositol phosphorylceramide (16–19).

In addition to these biosynthetic routes, complex sphingolipids, ceramide, and LCBs are also subject to degradation. Complex sphingolipids are cleaved by an inositol phosphosphingolipid phospholipase C, *Isc1* (20). Ceramide, on the other hand, is degraded through alkaline ceramidases *Ydc1* and *Ypc1* (21, 22). Phosphorylated LCBs, finally, can be cleaved by a sphingosine-1-phosphate lyase, *Dpl1*, to ethanolamine phosphate and fatty aldehyde (23). The activity of components of this degradative branch, *Isc1*, *Ydc1*, and *Ypc1*, is controlled by the target of rapamycin complex 1

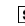
Abbreviations: CerS, ceramide synthase; DHS, dihydrosphingosine; ER, endoplasmic reticulum; LCB, long-chain base; OD, optical density; PHS, phytosphingosine; SPT, serine palmitoyl-CoA transferase; YPD, yeast peptone dextrose.

<sup>1</sup> Present address of F. Martínez-Montañés: Department of Biochemistry and Molecular Biology, University of Southern Denmark, 0230 Odense, Denmark.

<sup>2</sup> Present address of M. A. Lone: Institute for Clinical Chemistry, University Hospital Zurich, 8091 Zurich, Switzerland.

<sup>3</sup> To whom correspondence should be addressed.

e-mail: roger.schneider@unifr.ch

 The online version of this article (available at <http://www.jlr.org>) contains a supplement.

(24). Importantly, the transient intermediates of the pathway, LCB, LCB phosphate, and ceramide, not only act as biosynthetic precursors but also have important signaling functions in stress response (see Fig. 1A for an overview of the pathway) (25, 26).

Here we describe a novel LCB derivative, identified as an LCB vinyl ether. This LCB vinyl ether is generated mainly from PHS in cells that accumulate high levels of LCBs either due to deregulated de novo synthesis, a block in the degradative pathway, or uptake of externally provided PHS. Conversion of PHS to the vinyl ether derivative appears to act as a shunt for the catabolic pathway because PHS vinyl ether levels are greatly elevated in mutants that cannot phosphorylate LCBs or in mutants lacking the sphingosine-1-phosphate lyase. Consistent with a potential role in PHS detoxification, the PHS vinyl ether is excreted from cells.

## MATERIALS AND METHODS

### Yeast strains and growth conditions

Yeast strains and their genotypes are listed in supplemental Table S1. Strains were cultivated in yeast peptone dextrose (YPD)-rich medium (1% Bacto yeast extract, 2% Bacto peptone; US Biological, Swampscott, MA) or synthetic dextrose medium lacking uracil (SD-URA) synthetic medium (0.67% yeast nitrogen base without amino acids; US Biological, Salem, MA), 2% glucose, and the following amino acids: 20 mg/l of each adenine, arginine, histidine, methionine, and tryptophan; 60 mg/l leucine, 230 mg/l lysine, and 300 mg/l threonine. Double-mutant strains were generated by crossing of single mutants and by gene disruption, using PCR deletion cassettes and a marker rescue strategy (27). Myriocin (Sigma Aldrich, St. Louis, MO) was diluted in DMSO and used from a 1,000 $\times$  stock, and Fumonisin B1 (Enzo Life Sciences, Farmingdale, NY) was diluted in water and used from a 5 $\times$  stock. Sphingosine, 1-deoxysphinganine, C18-D-erythro-DHS, C2-dihydroceramide, C17/C18-DHS, and C17/C18-PHS were obtained from Avanti (Avanti Polar Lipids, Alabaster, AL); 1-threo-DHS and 2-deoxyglucose were from Sigma.

### Lipid extraction and analysis by MS

For lipid analysis, overnight cultures of strains were diluted into fresh YPD (Figs. 1B, 2, 3, 4, 5A, 7A) or SD-URA (Fig. 5B, 6B, 7B) media, and cells were grown at 30°C to an optical density (OD)<sub>600nm</sub> of approximately 2. Temperature-sensitive strains were grown at 24°C in YPD (Fig. 7A). Lipids were extracted from 10 OD<sub>600nm</sub> units of cells with CHCl<sub>3</sub> and methanol (2:1 by volume) or from the culture supernatant with 2 vol of diethyl ether. C17-DHS (1 nmol) was used as internal standard (28). LCBs were analyzed in the positive ion mode on a Bruker Esquire HCT ion trap mass spectrometer using ESI at a flow rate of 180 ml/h and a capillary tension of 250 V. Ion fragmentation was induced by argon case collision at a pressure of 8 mbar. [M + H]<sup>+</sup> ions of DHS, PHS, and the corresponding vinyl ether derivatives were quantified relative to the internal standard. Statistical significance of data was analyzed by a multiple *t*-test (GraphPad Prism, La Jolla, CA).

### Structural characterization of the vinyl ether by high-resolution MS

Structural identification using low-energy collision-induced dissociation (CID) linear ion trap (LIT) MS<sup>n</sup> with high-resolution ( $R = 100,000$  at  $m/z$  400) MS was conducted on a Thermo Scientific

(San Jose, CA) LTQ Orbitrap Velos mass spectrometer with Xcalibur operating system. Purified compound in methanol was infused (1.5  $\mu$ l/min) to the ESI source, where the skimmer was set at ground potential, the electrospray needle was 4.0 kV, and temperature of the heated capillary was set at 300°C. The automatic gain control of the ion trap was set to  $5 \times 10^4$ , with a maximum injection time of 50 ms. Helium was used as the buffer and collision gas at a pressure of  $1 \times 10^{-3}$  mbar (0.75 mTorr). The MS<sup>n</sup> experiments were carried out with an optimized relative collision energy ranging from 20% to 35% with an activation *q* value of 0.25 and the activation time of 10 ms to leave a minimal residual abundance of precursor ion ( $\sim 20\%$ ). The mass selection window for the precursor ions was set at 1 Da wide to admit the monoisotopic ion to the ion-trap for CID for unit resolution detection in the ion-trap or high-resolution accurate mass detection in the Orbitrap mass analyzer. Mass spectra were accumulated in the profile mode, typically for 2 to 10 min for MS<sup>n</sup> spectra ( $n = 2,3,4$ ).

## RESULTS AND DISCUSSION

### Identification and characterization of a PHS vinyl ether

In the course of analyzing LCB levels by MS in lipid extracts from various yeast mutants, we noticed an uncharacterized peak at  $m/z$  344.3. This lipid was of low abundance in wild-type cells (25 pmol/OD), but its concentration was greatly elevated in *elo3* $\Delta$  mutant cells (436 pmol/OD; Fig. 1B, C). *Elo3* is a component of the ER-associated acyl chain elongase complex required for the synthesis of C26 very long-chain fatty acids (29, 30). *elo3* $\Delta$  mutant cells make C22 instead of the normal C26 fatty acids. Shorter acyl-CoAs, however, are a poor substrate for CerS, the enzyme that catalyzes the *N*-acylation of LCBs to form ceramide (31, 32). As a consequence, *elo3* $\Delta$  mutant cells display greatly elevated levels of PHS. While wild-type cells have about 19 pmol/OD of PHS, *elo3* $\Delta$  mutant cells have up to 451 pmol/OD of PHS. The fact that the relative abundance of the lipid at  $m/z$  344.3 correlated with the abundance of PHS in wild-type and *elo3* $\Delta$  mutant cells suggested that it might be derived from PHS.

To test this hypothesis, we characterized the structure of this lipid by high-resolution MS. When subjected to ESI in the positive-ion mode, [M + H]<sup>+</sup> ions were observed at  $m/z$  344.3164, which corresponds to an elemental composition of C<sub>20</sub>H<sub>42</sub>O<sub>3</sub>N (calculated  $m/z = 344.3159$ ). In the negative-ion mode, ions at  $m/z$  342.3014, corresponding to an elemental composition of C<sub>20</sub>H<sub>40</sub>O<sub>3</sub>N (calculated  $m/z = 342.3013$ ), were observed. These results indicate that the compound had an elemental composition of C<sub>20</sub>H<sub>41</sub>O<sub>3</sub>N, representing a 1-*O*-ethenyl-2-amino-4-octadecene-1,3-diol, that is a PHS derivative containing a vinyl ether at the C1 hydroxyl group of PHS (Fig. 2).

Fragmentation (MS<sup>2</sup>) of the [M + H]<sup>+</sup> ions at  $m/z$  344.3164 gave rise to ions of 326 and 308, arising from consecutive losses of water (Fig. 2A, route a), along with ions of  $m/z$  300 arising from loss of CH<sub>2</sub>=CHOH, and ions of  $m/z$  282 (300 - H<sub>2</sub>O), arising from an additional loss of water (supplemental Fig. S1). Two pathways leading to the elimination of CH<sub>2</sub>=CHOH are proposed. The first pathway involves the participation of the hydrogen of the 3-OH group to

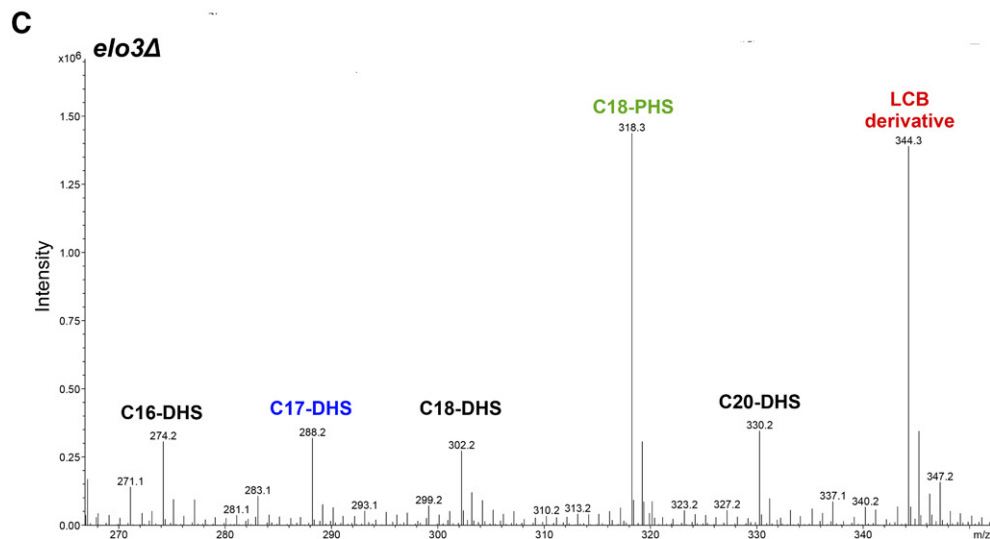
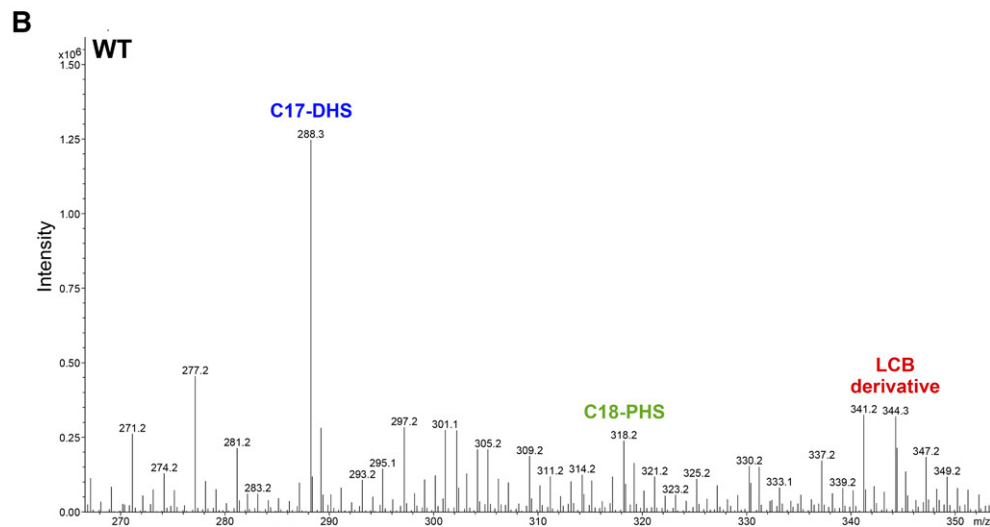
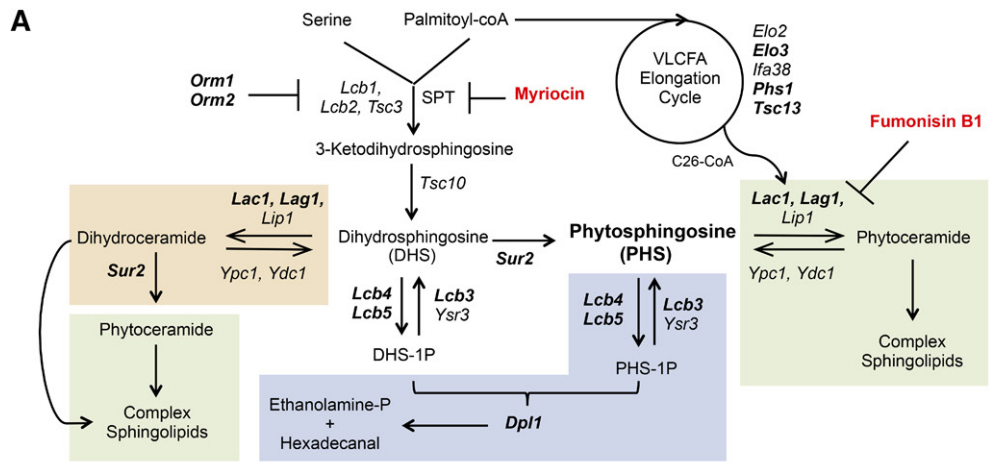


**Fig. 1.** Identification of a putative LCB derivative. **A:** Schematic overview of the yeast sphingolipid biosynthetic and degradative pathways. Key enzymes and lipid intermediates are shown. Mutants used in this study are indicated in bold, and drugs that were used are shown in red. The pathway leading to dihydroceramide is highlighted in orange, the maturation of phytoceramide to the complex sphingolipids is highlighted in green, and the degradative pathway is highlighted in blue. **B, C:** ESI/MS profile of LCBs present in wild-type (WT; **B**) and *elo3Δ* (**C**) mutant cells. Lipid extracts prepared from wild-type and elongase (*elo3Δ*) mutant cells were analyzed by ESI/MS in the positive ion mode using the odd chain-length C17-DHS ( $m/z$  288.3) as internal standard (indicated in blue). The major PHS species present in both strains, C18-PHS ( $m/z$  318.3) is indicated in green. The  $[M + H]^+$  ion at  $m/z$  344.3, indicated in red, represents a putative novel LCB derivative.

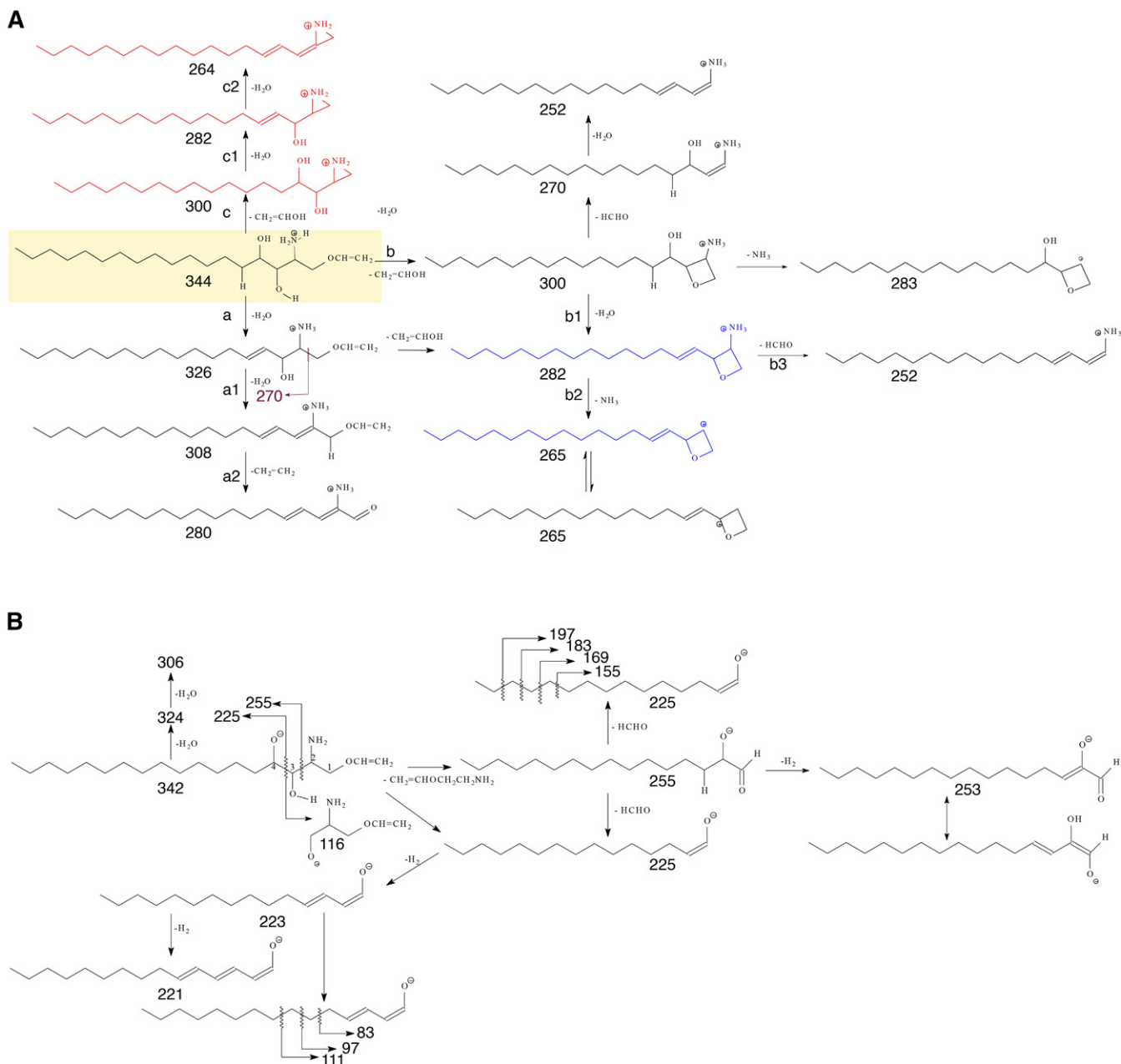


**Fig. 2.** High-resolution MS and fragmentation analysis indicate that the putative LCB derivative is a LCB vinyl ether. Lipid extract from *elo3Δ* mutant cells were subject to high-resolution MS and MS<sup>n</sup> analysis. A: Fragmentation scheme of the putative LCB derivative [M + H]<sup>+</sup> at *m/z* 344.3 in the positive ion mode. The structure of the LCB vinyl ether is highlighted in yellow, and the structures and *m/z* of the observed product ions are indicated by the arrows. Fragmentation along route c gives rise to the structures indicated in orange, and fragmentation along routes b1 and b2 gives rise to the structure indicated in blue. B: Fragmentation scheme of the putative LCB derivative [M - H]<sup>-</sup> at *m/z* 342.3 in the negative ion mode.

form a long alkyl chain with a terminal oxetane species of *m/z* 300 (Fig. 2A, route b), which gave rise to ions of *m/z* 282 via further loss of water (Fig. 2A, route b1). The second pathway involves the hydrogen of the secondary amino group, leading to the formation of an alkyl chain with a terminal aziridine (Fig. 2A, route c), which undergoes further loss of water to yield ions of *m/z* 282 (Fig. 2A, route c1). These fragmentation pathways were further supported by MS<sup>3</sup> spectrum of the ions of *m/z* 282 (344 → 282; supplemental Fig. S1B), which is identical to the MS<sup>4</sup> spectrum of *m/z* 282 (344 → 326 → 282; data not shown). The spectrum

(supplemental Fig. S1B) also contained ions of *m/z* 265 and 252 arising from losses of NH<sub>3</sub> (Fig. 2A, route b2, structures highlighted in blue) and HCHO (Fig. 2A, route b3), respectively. The ion of *m/z* 264 is a hallmark of the sphingosine LCB structure and arises from loss of water from the aziridine precursor ions (Fig. 2A, route c2, structures highlighted in orange) (33, 34). The above fragmentation processes were supported by high resolution MS, from which the deduced elemental composition of the fragment ions are consistent with the suggested structures (data not shown).

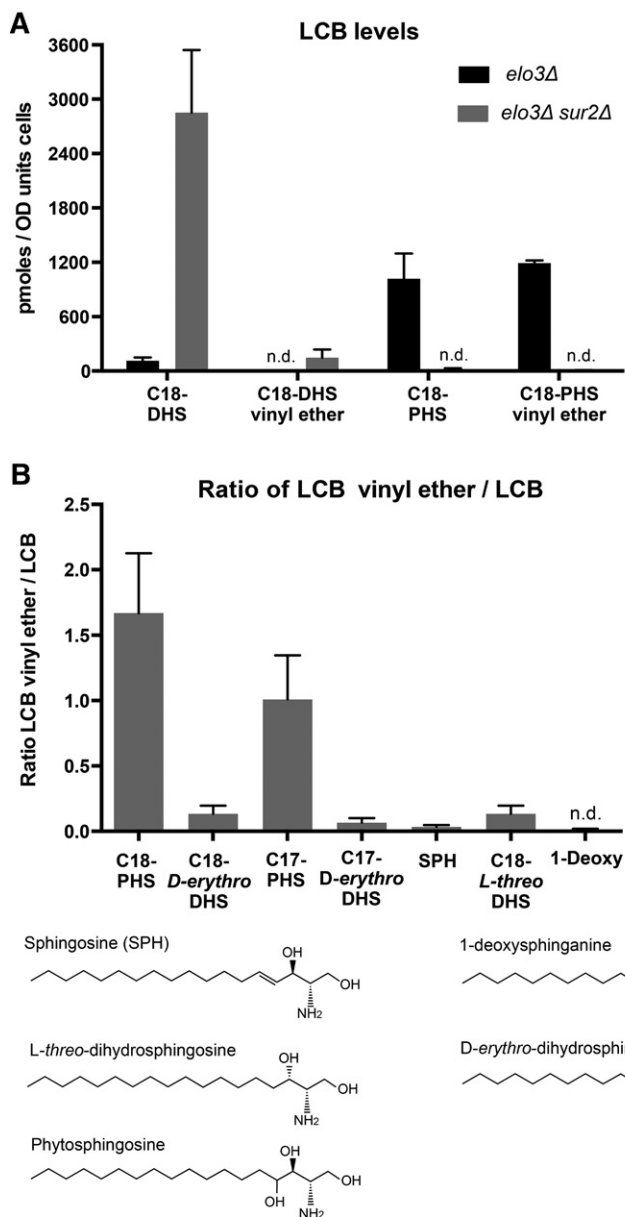


**Fig. 3.** The LCB vinyl ether is predominantly produced from PHS. A: PHS but not DHS is efficiently converted to the vinyl ether derivative. Lipids were extracted from *elo3Δ* and *elo3Δ sur2Δ* double mutant cells and LCBs were analyzed by ESI/MS with C17-DHS as an internal standard. *elo3Δ* mutant cells have about equimolar levels of both PHS and PHS vinyl ether. *elo3Δ sur2Δ* double mutant cells accumulate high levels of DHS but show only low levels of the corresponding DHS vinyl ether. B: Externally added PHS but not DHS is efficiently converted to the PHS vinyl ether. Wild-type cells were grown to OD ~2 and supplemented with 10  $\mu$ M of the indicated LCB for 30 min, lipids were extracted and analyzed by ESI/MS. The ratio of the externally added LCB to the corresponding vinyl ether derivative is blotted. Values represent means  $\pm$  SD of three independent determinations. n.d.; not detectable.

The structural assignment was further supported by high resolution LIT MS<sup>n</sup> of the corresponding  $[M - H]^-$  ions (Fig. 2B). The MS<sup>2</sup> spectrum of the  $[M - H]^-$  ion at  $m/z$  342 contained ions at  $m/z$  324 and 306 arising from consecutive losses of water, and prominent ions of  $m/z$  255, arising from cleavage of C<sub>3</sub>(OH)-C<sub>2</sub>(NH<sub>2</sub>) bond of the LCB, together with ions of  $m/z$  225 arising from cleavage of the C<sub>3</sub>(OH)-C<sub>4</sub>(OH) bond (35) (supplemental Fig. S2A). The cleavage of this latter bond is consistent with the formation of the ions of  $m/z$  116, in which the anionic charge site is located at the oxygen atom attached to C3 of the LCB (Fig. 2B). The presence of the ions of  $m/z$  116 also supports the notion of the presence of the 1-*O*-ethenyl group in the molecule. Further dissociation of the ions of  $m/z$  255 (342  $\rightarrow$  255; supplemental Fig. S2B) gave rise to the terminally conjugated ions of  $m/z$  253 via loss of H<sub>2</sub>, the prominent ions of  $m/z$  225 arising from loss of HCHO, and ions of  $m/z$  237 by loss of water. The MS<sup>4</sup> spectrum of the ions of  $m/z$  225 (342  $\rightarrow$  255  $\rightarrow$  225; supplemental Fig. S2C) are dominated

by ions of  $m/z$  223 and 221 representing a terminally conjugated diene and triene, respectively, arising from consecutive losses of H<sub>2</sub>. The spectrum also contained ions at  $m/z$  197, 183, 169, 155, and so forth, and at  $m/z$  111, 97, 83, arising from cleavages of the C-C bond of the LCB via charge-remote fragmentation (Fig. 2B). These results are consistent with the assignments of the suggested structure of 1-*O*-ethenyl-2-amino-4-octadecene-1,3-diol.

We note that the structure of the proposed PHS vinyl ether has the same elemental composition as C2-dihydroceramide and is thus isobaric with C2-dihydroceramide. The fragmentation pattern of the PHS vinyl ether in both positive and negative ion mode, however, is clearly distinct from that of C2-dihydroceramide (supplemental Fig. S3). Fragmentation of acetylated LCBs typically results in a characteristic loss of  $m/z$  42, corresponding to the loss of a ketene (supplemental Fig. S3). This is not observed upon fragmentation of PHS vinyl ether, which instead loses a fragment of  $m/z$  44, corresponding to a vinyl alcohol. Thus,

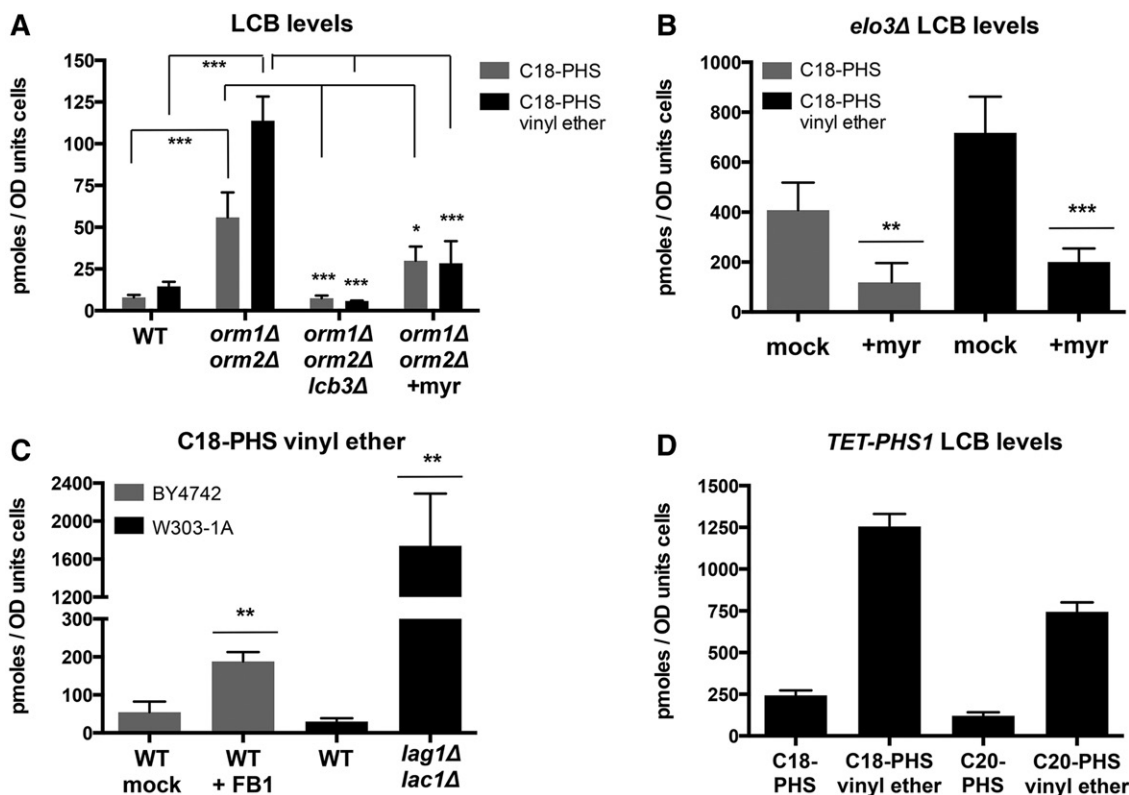


**Fig. 4.** Elevated levels of PHS provoke the accumulation of PHS vinyl ether. **A:** Mutants that accumulate high levels of PHS also display high levels of the vinyl ether derivative. Lipids were extracted from cells of the indicated genotypes and LCB levels were quantified by ESI/MS. For the myriocin treatment, *orm1Δ orm2Δ* double mutant cells were incubated with 1  $\mu\text{g}/\text{ml}$  myriocin for 4 h. **B:** Inhibition of SPT activity by myriocin leads to a simultaneous decrease in free PHS and PHS vinyl ether levels. *elo3Δ* mutant cells were treated with 5  $\mu\text{g}/\text{ml}$  myriocin for 4 h, and LCB levels were quantified by ESI/MS. **C:** Pharmacologic and genetic disruption of ceramide synthesis results in elevated levels of PHS vinyl ether. Wild-type cells were treated with 200  $\mu\text{M}$  of fumonisins B1, an inhibitor of CerS, for 4 h, and PHS vinyl ether levels were quantified by ESI/MS. *lag1Δ lac1Δ* double mutants lacking two components of the CerS have elevated levels of PHS vinyl ether. **D:** Conditional mutants in fatty acid elongation display elevated levels of C18- and C20-chain length PHS vinyl ethers. Cells that express the essential 3-hydroxyacyl-CoA dehydratase, *PHS1*, from a tetracycling repressible promoter (*TET-PHS1*) were cultivated in rich media, in which the promoter is only weakly active, lipids were extracted, and LCB levels quantified by ESI/MS. Values represent means  $\pm$  SD of three independent determinations. Asterisks denote statistical significance (\*  $P < 0.05$ ; \*\*  $P < 0.001$ ; \*\*\*  $P < 0.0001$ ).

the fragmentation pattern of the PHS vinyl ether is not compatible with that of either an *N*- or *O*-acetylated LCB, including C2-dihydroceramide.

#### PHS is efficiently converted to PHS vinyl ether

To confirm this structural assignment and to test whether DHS could also be converted to a DHS vinyl ether, we analyzed the formation of the LCB vinyl ether in cells that cannot form PHS due to a deletion of the *Sur2* hydroxylase, which converts DHS into PHS (36). Compared with *elo3Δ* mutant cells, the *elo3Δ sur2Δ* double mutant had greatly elevated levels of DHS. Despite these elevated DHS levels, the *elo3Δ sur2Δ* double mutant produces only very low levels of the corresponding DHS vinyl ether. PHS, accumulating in the *elo3Δ* single mutant, however, is efficiently converted to the PHS vinyl ether as *elo3Δ* mutant cells display about equal levels of both PHS and PHS vinyl ether (Fig. 3A). We thus conclude that PHS rather than DHS is the preferred substrate for formation of the LCB vinyl ether.

To test whether conversion of PHS to the vinyl ether derivative is a general reaction of cells to high levels of PHS, we challenged wild-type cells with externally added LCBs.

Wild-type cells incubated with 10  $\mu\text{M}$  PHS during 30 min displayed high levels of PHS vinyl ether. In these cells, levels of PHS vinyl ether were  $\sim 1.7$ -fold higher than free PHS levels (Fig. 3B). Cells incubated with DHS, however, displayed only low levels of the DHS vinyl ether, supporting the conclusion that PHS is the preferred substrate for formation of the LCB vinyl ether.

To distinguish between the conversion of internally synthesized LCBs and that of externally added LCBs to the vinyl ether, we challenged cells with a synthetic, odd chain length LCB tracer. We have previously shown that these C17-LCBs are efficiently taken up and incorporated into ceramide and complex sphingolipids (28). Wild-type cells converted C17-PHS efficiently to the C17-PHS vinyl ether, whereas C17-DHS was only inefficiently transformed to the C17-DHS vinyl ether (Fig. 3B). Other LCBs, such as sphingosine, or the stereoisomer of the natural DHS, *L*-threo-DHS, were also only very inefficiently converted to the corresponding vinyl ether derivatives. Deoxysphinganine, on the other hand, was not converted to the vinyl ether, which is consistent with the fact that the vinyl ether group is bound to the C1 hydroxyl group, which is missing in deoxysphinganine. Taken together, these results thus show

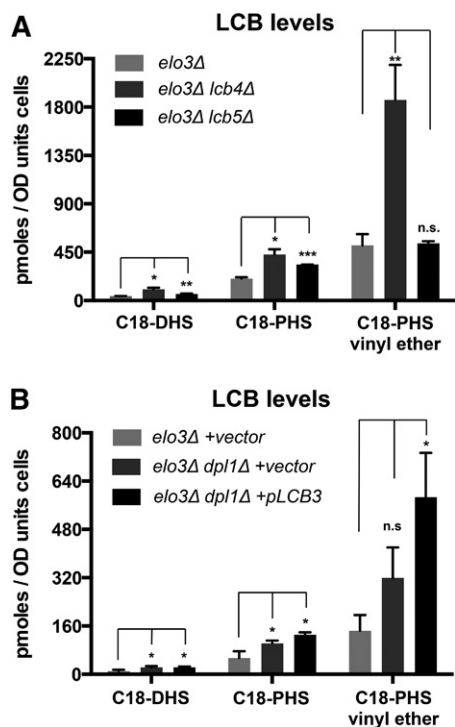


**Fig. 5.** Blocking the degradation of either free or phosphorylated LCBs results in the overaccumulation of PHS vinyl ether. A: *elo3Δ* mutant cells and double mutants of *elo3Δ* with either the major LCB kinase, *lcb4Δ*, or the minor kinase, *lcb5Δ*, were grown overnight to mid exponential phase in YPD media, lipids were extracted, and the indicated LCB levels were quantified by ESI/MS. B: *elo3Δ* mutant cells and *elo3Δ dpl1Δ* double mutant cells, lacking the LCB phosphate lyase, carrying either an empty vector (+vector) or a plasmid overexpressing the LCB phosphatase *LCB3* (+pLCB3) were grown in selective media, lipids were extracted, and LCB levels were quantified. Values represent means  $\pm$  SD of three independent determinations. Asterisks denote statistical significance with respect to *elo3Δ* mutant cells (\*  $P < 0.05$ ; \*\*  $P < 0.001$ ; \*\*\*  $P < 0.0001$ ). n.s.; not significant.

that both internally as well as externally provided PHS are efficiently converted to the vinyl ether and that the levels of free PHS and those of PHS vinyl ether reach similar levels irrespective of whether PHS is endogenously synthesized or whether it is taken up by the cells. DHS, on the other hand, is not efficiently converted to the DHS vinyl ether, indicating that the converting enzyme(s) has high substrate specificity for PHS over DHS.

### PHS vinyl ether levels parallel those of free PHS

To test whether mutants other than *elo3Δ* known to accumulate high levels of internal PHS also show elevated levels of PHS vinyl ether, we analyzed the levels of these two LCBs in mutants that have deregulated SPT activity. Orm proteins are conserved integral membrane proteins of the ER that negatively regulate SPT activity and *orm1Δ orm2Δ* double mutants show greatly increased LCB levels (7, 8). Consistent with this notion, the *orm1Δ orm2Δ* double mutant had greatly elevated levels of both PHS and PHS vinyl ether (Fig. 4A). Deletion of the LCB-phosphate phosphatase, *Lcb3*, in the *orm1Δ orm2Δ* double mutant has previously been shown to rescue the *orm* mutant from the detrimental accumulation of PHS (8). *Lcb3* is an ER-localized

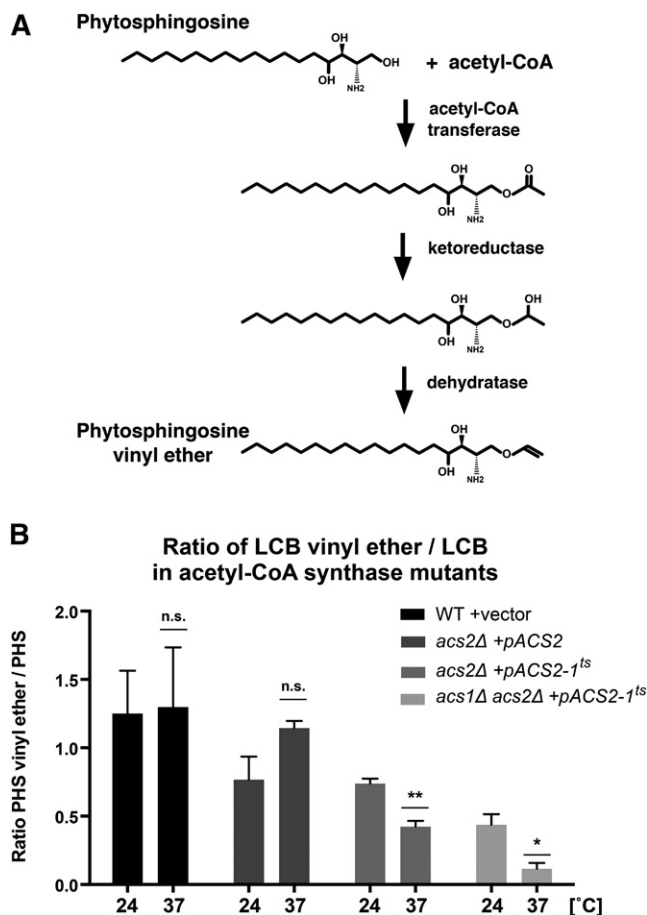


**Fig. 6.** PHS vinyl ether synthesis depends on acetyl-CoA production. A: Possible reaction sequence for the biosynthesis of a PHS vinyl ether, starting with an acetylated PHS, which is stepwise reduced to the vinyl ether derivative. B: Acetyl-CoA synthesis is required for synthesis of the PHS vinyl ether. Wild-type and acetyl-CoA synthase mutants (*acs2Δ*, *acs1Δ acs2Δ*) carrying either an empty vector (+vector) or a plasmid-borne wild-type copy of *ACS2* (+pACS2) or a temperature-sensitive allele (+pACS2-1<sup>ts</sup>) were grown at 24°C or shifted to 37°C for 2 h. Cells were incubated with 10  $\mu$ M C18-PHS for 30 min, and LCBs were extracted and quantified. Values represent means  $\pm$  SD of three independent determinations. Asterisks denote statistical significance (\*  $P < 0.05$ ; \*\*  $P < 0.001$ ; \*\*\*  $P < 0.0001$ ). n.s.; not significant.

phosphatase that dephosphorylates exogenously imported LCB phosphates, and this activity is necessary for the incorporation of exogenous LCBs into sphingolipids (21, 37–39). Levels of free PHS and those of PHS vinyl ether were reduced to wild-type concentrations upon deletion of *Lcb3* in the *orm1Δ orm2Δ* double mutant (Fig. 4A). Similarly, upon inhibition of SPT activity by myriocin, both PHS and PHS vinyl ether levels were significantly reduced in both *orm1Δ orm2Δ* and *elo3Δ* mutant cells (Fig. 4A, B).

Consistent with the notion that levels of the vinyl ether parallel those of the free PHS, wild-type cells treated with the CerS inhibitor fumonisin B1, which results in increased PHS levels, displayed a slight but significant increase in PHS vinyl ether levels (28) (Fig. 4C). Deletion of the catalytic components of the CerS, *Lag1* and *Lac1*, on the other hand, resulted in very high levels of PHS vinyl ether, consistent with the fact that *lag1Δ lac1Δ* double mutant cells have high levels of free PHS (14) (Fig. 4C). Repression of the

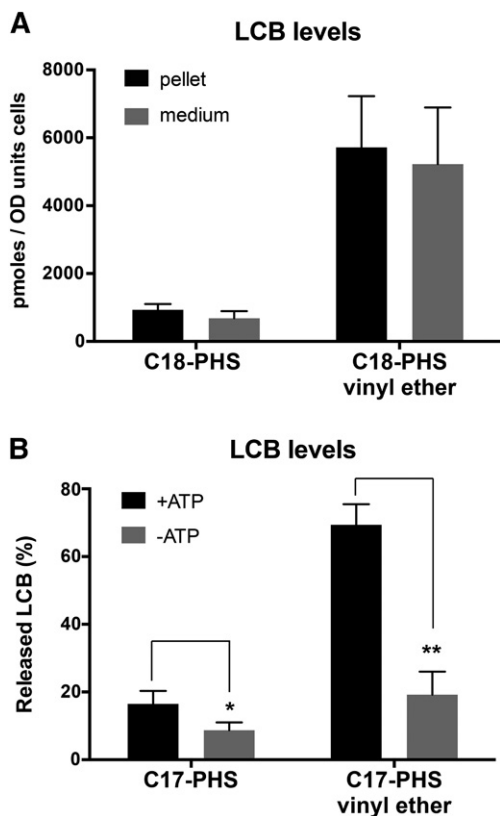


**Fig. 7.** The LCB vinyl ether is actively exported into the culture medium. **A:** A substantial fraction of PHS vinyl ether is excreted into the culture medium. PHS and PHS vinyl ether levels were quantified in the cell pellet and the culture supernatant of *tsc13-1 elo3Δ* double mutant cells. **B:** Export of PHS and PHS vinyl ether is energy dependent. *dpl1Δ* mutant cells overexpressing the putative LCB transporter, *RSBI*, were incubated with 10  $\mu$ M of C17-PHS for 20 min, cells were washed in media containing 1 mg/ml defatted BSA, and ATP levels were depleted by switching cells to medium containing 2-deoxyglucose instead of glucose and  $\text{NaN}_3/\text{NaF}$  (10 mM) for 15 min. Lipids were then extracted and quantified from the cell pellet and the culture medium. Released LCB levels are expressed as percentage of total LCBs. Asterisks denote statistical significance (\*  $P < 0.05$ ; \*\*  $P < 0.001$ ; \*\*\*  $P < 0.0001$ ). n.s.; not significant.

essential component of the acyl chain elongase, *PHS1*, which codes for a 3-hydroxyacyl-CoA dehydratase, through a tetracycling regulatable promoter (*TET-PHS1*), again resulted in high levels of the C18-PHS vinyl ether and also showed high levels of both C20-PHS and the C20-PHS vinyl ether (30, 40, 41) (Fig. 4D). It is interesting to note that *lag1Δ lac1Δ* double mutant cells and *TET-PHS1* cells have previously been shown to accumulate abnormally polar ceramides, as shown by TLC analysis of lipids labeled with [ $^3\text{H}$ ]DHS or [ $^{14}\text{C}$ ]serine (14, 15, 41). Given the very high levels of PHS vinyl ether produced in these cells, it is possible that the lipids identified as ceramide in these studies actually was the PHS vinyl ether. The presence of the vinyl ether group renders PHS so hydrophobic that it migrates close to ceramide (our unpublished observations).

Taken together, these results indicate that the levels of the vinyl ether consistently parallel those of the free PHS under the various conditions tested here, indicating that the half-life of the two lipids are similar, arguing thus against

the possibility that the vinyl ether acts as an inert storage form for the free LCB. In addition, the fact that LCBs of different chain length are converted to the respective vinyl ether indicates that the converting enzymes do not discriminate between these chain length variants of PHS.

#### PHS vinyl ether formation acts in parallel to the degradative pathway

LCBs enter the degradative pathway by first being phosphorylated by either *Lcb4* or *Lcb5*, the two LCB kinases in yeast. *Lcb4* is the major kinase located in the ER, whereas *Lcb5* has only minor activity in exponentially growing cells (42, 43). The resulting LCB-phosphates (LCB-P) can then either be dephosphorylated by *Lcb3/Ysr3* or they are cleaved by the LCB-P lyase, *Dpl1*, to ethanolamine phosphate and 1-hexadecanal (23). To test whether formation of the vinyl ether depends on prior phosphorylation of the LCB or whether it acts in parallel to this catabolic pathway, we analyzed LCB levels in double mutants of *elo3Δ* with either *lcb4Δ* or *lcb5Δ*. Deletion of these LCB kinases in the *elo3Δ* mutant background resulted in slightly elevated levels of DHS and PHS (Fig. 5A). Deletion of the main LCB kinase, *Lcb4*, in the *elo3Δ* mutant background, however, resulted in a dramatic accumulation of PHS vinyl ether, suggesting that a block in the catabolic pathway shunts PHS toward the formation of the vinyl ether derivative. Deletion of the minor kinase activity, *Lcb5*, on the other hand, did not significantly increase vinyl ether levels (Fig. 5A).

Given that blocking the degradative pathway through deletion of the major LCB kinase *Lcb4* resulted in greatly elevated levels of PHS vinyl ether, we examined whether deletion of the lyase would lead to a similar increase in PHS vinyl ether levels. Deletion of *Dpl1* in an *elo3Δ* mutant background again gave rise to slightly elevated levels of DHS and PHS; PHS vinyl ether levels, however, were not significantly increased. Upon overexpression of the LCB phosphate phosphatase, *Lcb3*, however, PHS vinyl ether levels became significantly elevated (Fig. 5B). Overexpression of *Lcb3* is expected to reduce the efficiency of the degradative pathway and hence to further increase levels of free LCBs. The fact that this resulted in accumulation of PHS vinyl ether is thus consistent with a shunt function of the pathway, which diverges free PHS into formation of the vinyl ether.

Taken together, these data indicate that vinyl ether synthesis is independent of the degradative pathway and that it acts in parallel to the catabolic pathway, possibly as a shunt for the degradative pathway under conditions of great excess of free intracellular LCBs. In addition, this shunt is possibly important to prevent the detrimental accumulation of LCB-phosphate (44, 45). On the other hand, the presence of the vinyl group on the C1 hydroxyl shield this LCB derivative from phosphorylation and subsequent degradation through the lyase pathway.

#### PHS vinyl ether formation depends on ongoing acetyl-CoA synthesis

To examine how the PHS vinyl ether is synthesized, we hypothesized that PHS may first be acetylated and the ketone group may subsequently be reduced, first to the hydroxyl




and then to the vinyl ether (Fig. 6A). This hypothesis would predict that formation of PHS vinyl ether is decreased in cells that have low acetyl-CoA levels. Acetyl-CoA can be produced by at least three major pathways in yeast: through the mitochondrial pyruvate dehydrogenase (PDH) complex, through peroxisomal  $\beta$ -oxidation, and through the two acetyl-CoA synthetases, *Acs1* and *Acs2* (46–48). Under aerobic conditions and on glucose-containing media, *ACS2* is essential and *ACS1* and the  $\beta$ -oxidation genes, e.g., *POT1*, are repressed, and the *PDH* genes are not essential (46, 47, 49). To examine the requirement of acetyl-CoA for the conversion of PHS into PHS vinyl ether, we challenged wild-type and *acs* mutant cells with externally provided PHS and monitored the appearance of the vinyl ether. Wild-type and *acs2* $\Delta$  mutant cells carrying a plasmid borne copy of *ACS2* (*acs2* $\Delta$  + pACS2) displayed an essentially equimolar ratio between PHS and PHS vinyl ether (Fig. 6B). The *acs2* $\Delta$  mutant rescued by a temperature-sensitive (ts) allele of *ACS2* (*pACS2-1<sup>ts</sup>*) and the *acs1* $\Delta$  *acs2* $\Delta$  double mutant carrying the same ts allele of *ACS2*, however, displayed significantly decreased levels of PHS vinyl ether compared with free PHS. These data thus indicate that normal acetyl-CoA levels are required for the efficient conversion of free PHS into PHS vinyl ether and hence that vinyl ether formation may proceed through the formation of an *O*-acetylated LCB intermediate. It is interesting to note that acetylated LCBs are found in certain microorganisms, such as *Wickerhamomyces ciferrii* (50). However, deletion of the acetyltransferases implicated in the formation of the *W. ciferrii* acetylated LCBs, *SLI1* and *ATF2*, in *Saccharomyces cerevisiae* did not affect PHS vinyl ether synthesis (data not shown). In mammals, on the other hand, 3-*O*-acetyl-sphingosine is present in so called fast migrating forms of cerambrosides. They appear during myelinogenesis and may play critical functions in myelin structure and function (51). The possibility that PHS vinyl ether synthesis occurs through an acetylated intermediate renders its synthesis analogous to that of the mammalian ether containing glycerophospholipids, which occurs through the exchange of *sn-1* bound acyl group on dihydroxyacetone phosphate by an alkyl group. The resulting alkyl ether can then be further reduced to a vinyl ether, as typically found in the plasmalogens (52).

### The PHS vinyl ether is excreted into the culture medium

Given that a PHS vinyl ether is considerably more hydrophobic than PHS itself, we wondered whether synthesis of the vinyl ether derivative might be a means to detoxify the cells from the detrimental effects of high PHS levels. We thus analyzed PHS and PHS vinyl ether levels in the cell pellet and the culture supernatant of elongase double mutant cells, *tsc13-1 elo3* $\Delta$ , which have high levels of free PHS and PHS vinyl ether (Fig. 7A). *TSC13* encodes for the enoyl reductase that catalyzes the last step in each very long-chain fatty acid elongation cycle (53). Interestingly, PHS and PHS vinyl ether levels present in the cell pellet were similar to the levels of these two lipids present in the culture supernatant, indicating that both of these LCBs can be exported by the cells. PHS vinyl ether levels, however, far exceeded PHS levels in both the cell pellet and the culture supernatant,

consistent with a possible role of the PHS vinyl ether in PHS detoxification.

Because intra- and extracellular levels of both PHS and PHS vinyl ether were comparable, it is conceivable that export of these lipids occurs by passive, energy-independent transport pathways. PHS export, on the other hand, has previously been described to be ATP dependent and to rely on *Rsb1*, a seven transmembrane protein, whose overexpression rescues the LCB sensitivity of *dpl1* $\Delta$  mutant cells (54, 55). To examine the energy requirement of the export of the vinyl ether, we challenged *dpl1* $\Delta$  mutant cells overexpressing *RSB1* with C17-PHS for 20 min, switched cells to medium containing 2-deoxyglucose and  $\text{NaN}_3/\text{NaF}$  to deplete ATP levels for 15 min, and then analyzed C17-PHS and C17-PHS vinyl ether levels in the cell pellet and the culture supernatant. Levels of both C17-PHS and that of the C17-PHS vinyl ether in the extracellular medium dropped significantly upon energy depletion of the cells, consistent with the notion that the export of both of these LCBs is dependent on an active, energy-requiring process (Fig. 7B).

Taken together, the data presented here indicate that free PHS is efficiently converted to a PHS vinyl ether derivative. This conversion is dependent on acetyl-CoA levels, and both free PHS and PHS vinyl ether are efficiently excreted by the cells. Based on these observations, we propose that the synthesis of the vinyl ether containing LCB may act to reduce levels of endogenous free LCBs and thus relieve cells of the growth inhibition of these LCBs. In this model, PHS vinyl ether synthesis and its export may thus act as a detoxification pathway to reduce levels of endogenous PHS (Fig. 8). If this were correct, one would predict that unlike free PHS, the PHS vinyl ether would not be taken up by the cells. A prediction that can be tested once a synthetic PHS vinyl ether will be available. In any case, conversion of free PHS into the vinyl ether derivative provides an additional means to regulate and fine tune the levels of free LCBs and thus to sustain cell proliferation under adverse conditions. 

The authors thank J. D. Boeke and T. Dunn for mutant strains; S. Reddy Polu and S. Schürch for initial analysis of the compound; A. Conzelmann, T. Hornemann, and S. G. Gowda for helpful discussions; and S. Cottier for comments on the manuscript.

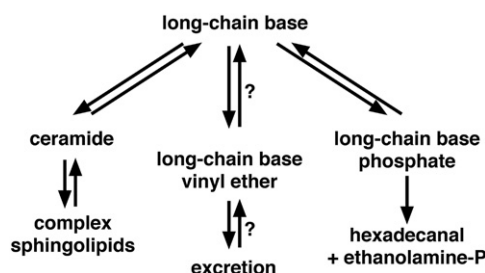


**Fig. 8.** Different fates of LCBs. Scheme summarizing the conversions of LCBs into ceramide, the vinyl ether derivative, and the phosphorylation-dependent catabolic pathway. The open questions of whether the LCB vinyl ether can be converted back into a free LCB and whether it can be efficiently taken up by the cells are indicated.

## REFERENCES

- Hannun, Y. A., and L. M. Obeid. 2008. Principles of bioactive lipid signalling: lessons from sphingolipids. *Nat. Rev. Mol. Cell Biol.* **9**: 139–150.
- Breslow, D. K., and J. S. Weissman. 2010. Membranes in balance: mechanisms of sphingolipid homeostasis. *Mol. Cell.* **40**: 267–279.
- Olson, D. K., F. Fröhlich, R. V. Farese, Jr., and T. C. Walther. 2016. Taming the sphinx: mechanisms of cellular sphingolipid homeostasis. *Biochim. Biophys. Acta.* **1861**: 784–792.
- Hanada, K. 2003. Serine palmitoyltransferase, a key enzyme of sphingolipid metabolism. *Biochim. Biophys. Acta.* **1632**: 16–30.
- Merrill, A. H. 2011. Sphingolipid and glycosphingolipid metabolic pathways in the era of sphingolipidomics. *Chem. Rev.* **111**: 6387–6422.
- Pruett, S. T., A. Bushnev, K. Hagedorn, M. Adiga, C. A. Haynes, M. C. Sullards, D. C. Liotta, and A. H. J. Merrill. 2008. Biodiversity of sphingoid bases (“sphingosines”) and related amino alcohols. *J. Lipid Res.* **49**: 1621–1639.
- Breslow, D. K., S. R. Collins, B. Bodenmiller, R. Aebersold, K. Simons, A. Shevchenko, C. S. Ejsing, and J. S. Weissman. 2010. Orm family proteins mediate sphingolipid homeostasis. *Nature.* **463**: 1048–1053.
- Han, S., M. A. Lone, R. Schneider, and A. Chang. 2010. Orm1 and Orm2 are conserved endoplasmic reticulum membrane proteins regulating lipid homeostasis and protein quality control. *Proc. Natl. Acad. Sci. USA.* **107**: 5851–5856.
- Roelants, F. M., D. K. Breslow, A. Muir, J. S. Weissman, and J. Thorner. 2011. Protein kinase Ypk1 phosphorylates regulatory proteins Orm1 and Orm2 to control sphingolipid homeostasis in *Saccharomyces cerevisiae*. *Proc. Natl. Acad. Sci. USA.* **108**: 19222–19227.
- Liu, M., C. Huang, S. R. Polu, R. Schneider, and A. Chang. 2012. Regulation of sphingolipid synthesis through Orm1 and Orm2 in yeast. *J. Cell Sci.* **125**: 2428–2435.
- Sun, Y., Y. Miao, Y. Yamane, C. Zhang, K. M. Shokat, H. Takematsu, Y. Kozutsumi, and D. G. Drubin. 2012. Orm protein phosphoregulation mediates transient sphingolipid biosynthesis response to heat stress via the Pkh-Ypk and Cdc55-PP2A pathways. *Mol. Biol. Cell.* **23**: 2388–2398.
- Gururaj, C., R. S. Federman, and A. Chang. 2013. Orm proteins integrate multiple signals to maintain sphingolipid homeostasis. *J. Biol. Chem.* **288**: 20453–20463. [Erratum. 2015. *J. Biol. Chem.* **290**: 1455.]
- Shimobayashi, M., W. Oppliger, S. Moes, P. Jenö, and M. N. Hal I. 2013. TORC1-regulated protein kinase Npr1 phosphorylates Orm to stimulate complex sphingolipid synthesis. *Mol. Biol. Cell.* **24**: 870–881.
- Guillas, I., P. A. Kirchman, R. Chuard, M. Pfefferli, J. C. Jiang, S. M. Jazwinski, and A. Conzelmann. 2001. C26-CoA-dependent ceramide synthesis of *Saccharomyces cerevisiae* is operated by Lag1p and Lac1p. *EMBO J.* **20**: 2655–2665.
- Schorling, S., B. Vallee, W. P. Barz, H. Riezman, and D. Oesterhelt. 2001. Lag1p and Lac1p are essential for the Acyl-CoA-dependent ceramide synthase reaction in *Saccharomyces cerevisiae*. *Mol. Biol. Cell.* **12**: 3417–3427.
- Dickson, R. C. 2008. Thematic review series: sphingolipids. New insights into sphingolipid metabolism and function in budding yeast. *J. Lipid Res.* **49**: 909–921.
- Puoti, A., C. Desponds, and A. Conzelmann. 1991. Biosynthesis of mannosylinositolphosphoceramide in *Saccharomyces cerevisiae* is dependent on genes controlling the flow of secretory vesicles from the endoplasmic reticulum to the Golgi. *J. Cell Biol.* **113**: 515–525.
- Funato, K., and H. Riezman. 2001. Vesicular and nonvesicular transport of ceramide from ER to the Golgi apparatus in yeast. *J. Cell Biol.* **155**: 949–959.
- Ejsing, C. S., J. L. Sampaio, V. Surendranath, E. Duchoslav, K. Ekroos, R. W. Klemm, K. Simons, and A. Shevchenko. 2009. Global analysis of the yeast lipidome by quantitative shotgun mass spectrometry. *Proc. Natl. Acad. Sci. USA.* **106**: 2136–2141.
- Sawai, H., Y. Okamoto, C. Luberto, C. Mao, A. Bielawska, N. Domae, and Y. A. Hannun. 2000. Identification of ISCL (YER019w) as inositol phosphosphingolipid phospholipase C in *Saccharomyces cerevisiae*. *J. Biol. Chem.* **275**: 39793–39798.
- Mao, C., M. Wadleigh, G. M. Jenkins, Y. A. Hannun, and L. M. Obeid. 1997. Identification and characterization of *Saccharomyces cerevisiae* dihydrosphingosine-1-phosphate phosphatase. *J. Biol. Chem.* **272**: 28690–28694.
- Mao, C., R. Xu, A. Bielawska, and L. M. Obeid. 2000. Cloning of an alkaline ceramidase from *Saccharomyces cerevisiae*. An enzyme with reverse (CoA-independent) ceramide synthase activity. *J. Biol. Chem.* **275**: 6876–6884.
- Saba, J. D., F. Nara, A. Bielawska, S. Garrett, and Y. A. Hannun. 1997. The BST1 gene of *Saccharomyces cerevisiae* is the sphingosine-1-phosphate lyase. *J. Biol. Chem.* **272**: 26087–26090.
- Swinnen, E., T. Wilms, J. Idkowiak-Baldys, B. Smets, P. De Snijder, S. Accardo, R. Ghillebert, K. Thevissen, B. Cammue, D. De Vos, et al. 2014. The protein kinase Sch9 is a key regulator of sphingolipid metabolism in *Saccharomyces cerevisiae*. *Mol. Biol. Cell.* **25**: 196–211.
- Epstein, S., and H. Riezman. 2013. Sphingolipid signaling in yeast: potential implications for understanding disease. *Front. Biosci. (Elite Ed.)* **5**: 97–108.
- Montefusco, D. J., N. Matmati, and Y. A. Hannun. 2014. The yeast sphingolipid signaling landscape. *Chem. Phys. Lipids.* **177**: 26–40.
- Guedener, U., J. Heinisch, G. J. Koehler, D. Voss, and J. H. Hegemann. 2002. A second set of loxP marker cassettes for Cre-mediated multiple gene knockouts in budding yeast. *Nucleic Acids Res.* **30**: e23.
- Martínez-Montañés, F., and R. Schneider. 2016. Following the flux of long-chain bases through the sphingolipid pathway in vivo using mass spectrometry. *J. Lipid Res.* **57**: 906–915.
- Oh, C. S., D. A. Toke, S. Mandala, and C. E. Martin. 1997. ELO2 and ELO3, homologues of the *Saccharomyces cerevisiae* ELO1 gene, function in fatty acid elongation and are required for sphingolipid formation. *J. Biol. Chem.* **272**: 17376–17384.
- Denic, V., and J. S. Weissman. 2007. A molecular caliper mechanism for determining very long-chain fatty acid length. *Cell.* **130**: 663–677.
- Guillas, I., J. C. Jiang, C. Vionnet, C. Roubaty, D. Uldry, R. Chuard, J. Wang, S. M. Jazwinski, and A. Conzelmann. 2003. Human homologues of LAG1 reconstitute Acyl-CoA-dependent ceramide synthesis in yeast. *J. Biol. Chem.* **278**: 37083–37091.
- Kobayashi, S. D., and M. M. Nagiec. 2003. Ceramide/long-chain base phosphate rheostat in *Saccharomyces cerevisiae*: regulation of ceramide synthesis by Elo3p and Cka2p. *Eukaryot. Cell.* **2**: 284–294.
- Kerwin, J. L., A. M. Wiens, and L. H. Ericsson. 1996. Identification of fatty acids by electrospray mass spectrometry and tandem mass spectrometry. *J. Mass Spectrom.* **31**: 184–192.
- Hsu, F. F., J. Turk, M. E. Stewart, and D. T. Downing. 2002. Structural studies on ceramides as lithiated adducts by low energy collisional-activated dissociation tandem mass spectrometry with electrospray ionization. *J. Am. Soc. Mass Spectrom.* **13**: 680–695.
- Hsu, F. F. 2016. Complete structural characterization of ceramides as [M - H]<sup>-</sup> ions by multiple-stage linear ion trap mass spectrometry. *Biochimie*. In press.
- Haak, D., K. Gable, T. Beeler, and T. Dunn. 1997. Hydroxylation of *Saccharomyces cerevisiae* ceramides requires Sur2p and Scs7p. *J. Biol. Chem.* **272**: 29704–29710.
- Qie, L., M. M. Nagiec, J. A. Baltisberger, R. L. Lester, and R. C. Dickson. 1997. Identification of a *Saccharomyces* gene, LCB3, necessary for incorporation of exogenous long chain bases into sphingolipids. *J. Biol. Chem.* **272**: 16110–16117.
- Mandala, S. M., R. Thornton, Z. Tu, M. B. Kurtz, J. Nickels, J. Broach, R. Menzelev, and S. Spiegel. 1998. Sphingoid base 1-phosphate phosphatase: a key regulator of sphingolipid metabolism and stress response. *Proc. Natl. Acad. Sci. USA.* **95**: 150–155.
- Kihara, A., T. Sano, S. Iwaki, and Y. Igarashi. 2003. Transmembrane topology of sphingoid long-chain base-1-phosphate phosphatase, Lcb3p. *Genes Cells.* **8**: 525–535.
- Hughes, T. R., M. J. Marton, A. R. Jones, C. J. Roberts, R. Stoughton, C. D. Armour, H. A. Bennett, E. Coffey, H. Dai, Y. D. He, et al. 2000. Functional discovery via a compendium of expression profiles. *Cell.* **102**: 109–126.
- Kihara, A., H. Sakuraba, M. Ikeda, A. Denpoh, and Y. Igarashi. 2008. Membrane topology and essential amino acid residues of Phs1, a 3-hydroxyacyl-CoA dehydratase involved in very long-chain fatty acid elongation. *J. Biol. Chem.* **283**: 11199–11209.
- Nagiec, M. M., M. Skrzypek, E. E. Nagiec, R. L. Lester, and R. C. Dickson. 1998. The LCB4 (YOR171c) and LCB5 (YLR260w) genes of *Saccharomyces* encode sphingoid long chain base kinases. *J. Biol. Chem.* **273**: 19437–19442.
- Funato, K., R. Lombardi, B. Vallee, and H. Riezman. 2003. Lcb4p is a key regulator of ceramide synthesis from exogenous long chain sphingoid base in *Saccharomyces cerevisiae*. *J. Biol. Chem.* **278**: 7325–7334.

44. Kim, S., H. Fyrst, and J. Saba. 2000. Accumulation of phosphorylated sphingoid long chain bases results in cell growth inhibition in *Saccharomyces cerevisiae*. *Genetics*. **156**: 1519–1529.
45. Zhang, X., M. S. Skrzypek, R. L. Lester, and R. C. Dickson. 2001. Elevation of endogenous sphingolipid long-chain base phosphates kills *Saccharomyces cerevisiae* cells. *Curr. Genet.* **40**: 221–233.
46. Pronk, J. T., H. Yde Steensma, and J. P. Van Dijken. 1996. Pyruvate metabolism in *Saccharomyces cerevisiae*. *Yeast*. **12**: 1607–1633.
47. Hiltunen, J. K., A. M. Mursula, H. Rottensteiner, R. K. Wierenga, A. J. Kastaniotis, and A. Gurvitz. 2003. The biochemistry of peroxisomal beta-oxidation in the yeast *Saccharomyces cerevisiae*. *FEMS Microbiol. Rev.* **27**: 35–64.
48. Starai, V. J., and J. C. Escalante-Semerena. 2004. Acetyl-coenzyme A synthetase (AMP forming). *Cell. Mol. Life Sci.* **61**: 2020–2030.
49. van den Berg, M. A., P. de Jong-Gubbels, C. J. Kortland, J. P. van Dijken, J. T. Pronk, and H. Y. Steensma. 1996. The two acetyl-coenzyme A synthetases of *Saccharomyces cerevisiae* differ with respect to kinetic properties and transcriptional regulation. *J. Biol. Chem.* **271**: 28953–28959.
50. Ter Veld, F., D. Wolff, C. Schorsch, T. Köhler, E. Boles, and A. Poetsch. 2013. Production of tetraacetyl phytosphingosine (TAPS) in *Wickerhamomyces ciferrii* is catalyzed by acetyltransferases Sli1p and Atf2p. *Appl. Microbiol. Biotechnol.* **97**: 8537–8546.
51. Dasgupta, S., S. B. Levery, and E. L. Hogan. 2002. 3-O-acetyl-sphingosine-series myelin glycolipids: characterization of novel 3-O-acetyl-sphingosine galactosylceramide. *J. Lipid Res.* **43**: 751–761.
52. Magnusson, C. D., and G. G. Haraldsson. 2011. Ether lipids. *Chem. Phys. Lipids*. **164**: 315–340.
53. Kohlwein, S. D., S. Eder, C. S. Oh, C. E. Martin, K. Gable, D. Bacikova, and T. Dunn. 2001. Tsc13p is required for fatty acid elongation and localizes to a novel structure at the nuclear-vacuolar interface in *Saccharomyces cerevisiae*. *Mol. Cell. Biol.* **21**: 109–125.
54. Kihara, A., and Y. Igarashi. 2002. Identification and characterization of a *Saccharomyces cerevisiae* gene, RSB1, involved in sphingoid long-chain base release. *J. Biol. Chem.* **277**: 30048–30054.
55. Panwar, S. L., and W. S. Moye-Rowley. 2006. Long chain base tolerance in *Saccharomyces cerevisiae* is induced by retrograde signals from the mitochondria. *J. Biol. Chem.* **281**: 6376–6384.